Teknik Dergi, 2022 12617-12634, Paper 697

Numerical Study on the Deformation Behavior of Geosynthetic-Encased Stone Columns Supporting Embankments

Tuncay DOĞAN[1]
Mehmet Rıfat KAHYAOĞLU[2]

ABSTRACT

The method of encasing the stone column with a proper type of geosynthetic material is a widely used technique to provide the required lateral confinement and to avoid the dispersion of granular column material into soft clay. Along with the improved ultimate load capacity and the reduced settlement and bulging, the geosynthetic encasement preserves the easy drainage ability of stone columns. This paper presents the finite element analysis results of a hypothetical embankment on a soft soil deposit which is improved by geotextile encased stone columns and geogrid reinforced sand mat on top. At first, numerical results of three dimensional (3D) finite element model (FEM) were validated via the experimental data of previous field studies. Afterward, parametric studies were carried out on the FEM considering the effect of the sand mat thickness, the stiffness of the geosynthetic reinforcement, and the geosynthetic encasing length and encasement stiffness on both the horizontal and vertical deformation of stone columns. Settlement differences between columns and soft soil in both the short term and long term were also determined. The optimum values of sand mat layer thickness, vertical encasement length, and geosynthetic stiffness are recommended to be used for preliminary designs.

Keywords: Stone column, geotextile encasement, geogrid reinforcement, sand mat, settlement, bulging.

1. INTRODUCTION

The use of column-supported embankments (CSEs) provides rapid construction, quicker consolidation, total and differential settlement reduction, and adjacent facility protection [1-2]. However, it appears to be impossible to improve very soft clayey soils with CSEs, due to

Note:
- This paper was received on June 8, 2021 and accepted for publication by the Editorial Board on February 18, 2022.
- Discussions on this paper will be accepted by November 30, 2022.
- https://doi.org/10.18400/tekderg.949826

1 Department of Civil Engineering, Muğla Sıtkı Koçman University, Muğla, Turkey
dogantuncay@msn.com - https://orcid.org/0000-0002-6376-2163

2 Department of Civil Engineering, Muğla Sıtkı Koçman University, Muğla, Turkey
rkahyaoglu@mu.edu.tr - https://orcid.org/0000-0002-9288-5277

lack of lateral confinement and excessive lateral bulging of column material [3]. In such types of soils, insufficient confinement requirements can be persuaded by encasing the column with the proper type of geosynthetics [4-5].

The impact of geosynthetic stiffness increment on ultimate load capacity improvement, settlement, and bulging reduction of geosynthetic encased columns (GECs), and excess pore water pressure change in the soft ground was investigated through the field and scaled laboratory experiments [6-9]. Murugesan and Rajagopal (2007) asserted that the most effective parameter of the instrumented GECs was the tensile strength of encasement. They also indicated that since the greatest radial geosynthetic strain occurs at the upper part, columns should be encased in the length of the 4-fold diameter [6]. Liu et al. (2007) published the in-situ results of a case study of basal geogrid reinforced and pile-supported highway embankment [7]. The measured pressure on the piles was measured to be 14-fold bigger than that on the soil. The study reveals that soil arching transfers the loads from soil to the piles hereby excess pore pressure reduces significantly. Murugesan and Rajagopal (2010) examined the influence of material properties and the geometry of the model for both encased and non-encased stone columns in a large-scale laboratory test setup and suggested design codes for specific load and settlement conditions [8]. Yoo et al. (2015) conducted loading tests on an artificially sedimented clay ground reinforced by geotextile-encased sand piles (GESP) and conventional sand compaction piles (SCP). Results show that the failure mode of SCPs is bulging where it is buckling for GESPs thus, the geosynthetic stiffness has nearly no effect on the load-carrying capacity in the buckling failure [9].

Moreover, there are countless accomplished samples of numerical studies on encased granular columns in the literature [10-11]. Murugesan and Rajagopal (2006) implied that the geosynthetic encased stone columns (GESCs) were stiffer than ordinary stone columns [10]. Yoo (2015) presented charts for preliminary design on the estimation of the ultimate vertical deformation and the stress concentration ratio (SCR) [11]. Tabesh and Poulos (2007) declared that constructing floating columns is more feasible in cases where the column tip cannot reach the rigid ground [12]. The frictional force along the column length affects the GESCs behavior, therefore the settlement differences between the pile and the surrounding ground should be considered [13].

In recent years, the horizontal (basal) geogrid reinforcement has found an area of utilization combined with column supported embankments (CSEs) over soft clay soils in circumstances of high embankment loads to create a geosynthetic reinforced column supported embankment (GRCSE) [14-15]. Cheng et al. (2014) examined the ultimate load capacity of a geosynthetic reinforced column supported (GRCS) platform by analyzing the 15-month long in-situ data. They revealed the possible generation of soil arching for certain heights of fill, that way the GRCS system can improve the stability of the embankment and reduce bulging significantly. The results proved that the usage of the geogrid reinforcement over the composite ground improves the transfer of loads from the embankment into the stone columns [16]. Liu et al. (2017) conducted parametric analyses on several factors such as pile spacing, coefficient of shear strength, internal friction angle, and cohesion of fill material in order to compare how they affect the load transfer behavior. The study points out that the cohesion is more effective than the internal friction angle of embankment fill on the load transfer mechanism [17].

The published literature focusing on the long-term vertical and lateral deformation behavior of geosynthetic encased stone columns (GESC) is limited. Many recent studies have dealt with the load-carrying capacities and settlements of unreinforced embankments supported

with GESCs. Nevertheless, the effect of reinforcement at the base of the embankment has not been considered yet. Furthermore, the load transfer mechanism and the bulging (lateral deformation) behavior of the GESCs are not thoroughly determined.

This paper interprets the findings of finite element analysis (FEA) results of a hypothetical geotextile-encased stone column-supported embankment which is improved by a geogrid reinforced sand mat (GRSM) in soft soil. To enhance the performance of GESCs and to fill the gaps for the above-mentioned issues, the main objectives of the present study can be listed briefly as; (1) to investigate the performance of vertical encasement on stone columns and the geosynthetic reinforcement at sand mat layer, (2) to determine the optimum sand mat layer thickness and the optimum geogrid reinforcement stiffness, (3) to determine the optimum vertical geotextile encasement stiffness (tensile strength) and the adequate length of the column encasement, (4) to consider the effect of geotextile encasement on the settlement (vertical displacement) and lateral deformation (bulging) behavior of stone columns.

2. NUMERICAL ANALYSIS AND PARAMETRIC STUDY

A hypothetical composite soil system was idealized and simulated with 3D FE analyses using PLAXIS 3D (Plaxis v.b 2018) [18]. First, the model was verified with the soft ground at the study of Raju (1997) [19]. Then, parametric studies on the load-carrying capacity and the deformation behavior of vertically encased columns were carried out for various parameters including the sand mat layer thickness, the stiffness of reinforcement, and encasement. The 3D FEM, FE mesh and cross-section of the model are shown in Fig. 1(a), Fig. 1(b) and Fig. 1(c).

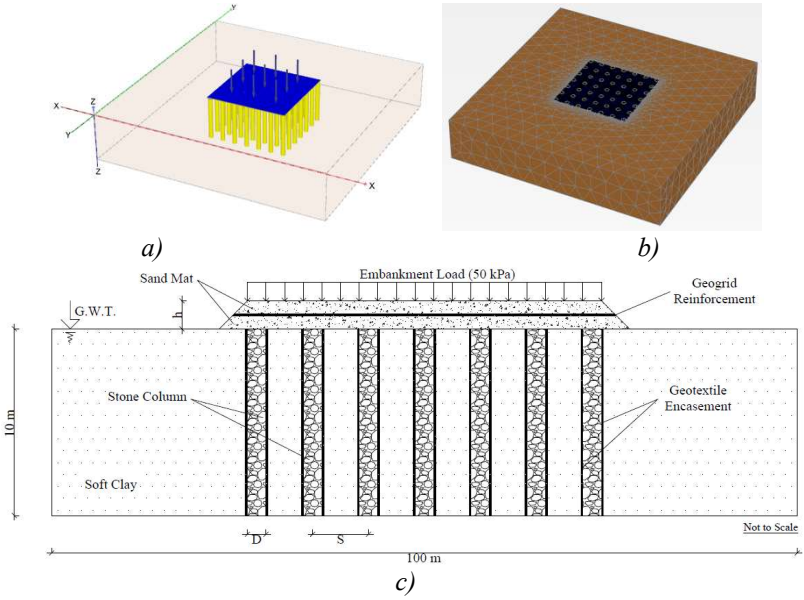

Fig. 1 - (a) 3D View of FEM, (b) FE Mesh of PLAXIS 3D Model, (c) Cross-Section of the Model

2.1. Material Properties

In this study, three types of soil materials have been used to simulate the soft ground, the sand mat, and the granular column. Known to be accurately corresponding to the behavior of the soft soil between columns, the Modified Cam-Clay (MCC) Model was used to simulate the ground in undrained condition, following the advice of Kaliakin et al. (2012) and Khabbazian et al. (2015) [20-21]. MCC model is defined by five parameters: the slope of the swelling line (K), the slope of the virgin consolidation line (λ), the void ratio at unit pressure (e), the slope of the critical state line (M), and Poisson's ratio (υ). Stone columns and the sand mat layer were modeled as granular soil and idealized by Mohr-Coulomb (MC) Model as a homogenous drained soil material [22]. Five material parameters are associated with this model, namely effective friction angle (ϕ′), effective cohesion (c′), dilation angle (φ′), elastic modulus (E), and Poisson's ratio (υ). The Mohr-Coulomb and the Modified Cam Clay parameters used in the numerical analyses were similar to typical values with the previous studies e.g. [11, 20, 22]. Detailed information about soft soil, sand mat layer, and stone column are given below (Table 1).

Table 1 - Material properties used in the numerical analyses

Parameter	**Column Material** *Stone / Soil* **[22]**	**Sand Mat Material** *Sacramento river sand* **[20]**	**Soft Clay Material** *Malaysian marine clay* **[23-25]**
Model type	MC	MC	MCC
Effective unit weight, ɣ′ (kN/m^3)	19	18	15
Effective friction angle, ϕ′(°)	43	32	-
Elastic modulus, E (kPa)	55000	15000	-
Poisson's ratio, υ	0.3	0.3	0.3
Effective cohesion, c′(kPa)	1	1	-
Permeability, k (m/s)	1x10^{-2}	1x10^{-3}	1x10^{-6}
Dilation angle, φ′(°)	10	3	-
Slope of the critical state line, M	-	-	1.0
Slope of the virgin cons. line, λ	-	-	0.4
Slope of swelling line, K	-	-	0.02
Void ratio at unit pressure, e	-	-	1.0

The geosynthetics used for both vertical encasement and basal reinforcement were modeled as linear elastic material with axial stiffness in elastic or elastoplastic forms, with an assumed Poisson's ratio of 0.30 e.g. [7]. The secant stiffness of the geosynthetic (J) was defined as the ratio of the tensile force per unit width to the average strain in the geosynthetic. The initial

tensile modulus was computed at 3% axial strain to determine the geosynthetic elastic module. Geosynthetic encasement design values for stone column were documented as required tensile modulus (J) between 1000 and 4000 kN/m by Almeida et al. (2015) [26]. Therefore, values between J=500-3500 kN/m were used in the numerical analyses for encasement. Also, seven different reinforcements with stiffness of J=1000-7000 kN/m were used to investigate the influence of the basal reinforcement.

In order to model the interaction behavior between the geosynthetic and the granular column, and between the geosynthetic and the surrounding soft soil, interface elements that can be characterized by two sets of parameters were used. The coefficient of sliding friction (μ) between the geosynthetic and the granular column was selected to be 0.5 ($\mu = 2/3 \tan\phi$) [27], where ϕ is the friction angle of the column material. For interaction between the geosynthetic and the soft soil, μ was assumed to be 0.3 ($\mu = 0.7 \tan\phi$) [28], where ϕ is the friction angle of the soft soil.

2.2. Geometry Model

In the analyses, the FE model limits were designated 100 m x 100 m in the horizontal direction and 10 m in the vertical direction. The stone column length and depth of the soft clay layer were adopted as 10 meters to simulate the fixed column behavior. Ordinary (conventional) stone columns (OSC) and vertically encased stone columns (VESC) with varying diameters of 0.60, 1.00, and 1.40 m and varying center-to-center column spacing ratios (s/D) of 2, 3, and 4 were selected within the analyses.

2.3. Model Verification

The case study by Raju (1997) in which a stone-column-supported embankment constructed in Kebun, Malaysia was adopted and simulated numerically with PLAXIS 3D [19]. The Kebun interchange is located near the city of Klang on the west coast of Malaysia. The upper soils in the coastal region are predominantly extremely soft marine clays having thicknesses of up to 35 m. and the very soft clay deposit is 11m thick in the cone test carried out in Kebun. Tip resistances range between 0.1 MPa and 0.3 MPa in the soft clay deposit. Undrained shear strengths as low as 5 kPa and an increasing rate of about 1 kPa per meter in depth have been measured. 1m high embankment on untreated soil has failed. At the site, only the typical values for moisture content (w), liquid limit (w_l), plastic limit (w_p), plasticity index (PI), clay, silt, and sand fractions, the sensitivity values (St), and the coefficient of consolidation (c_v) for the soft soils were encountered. Still, it is not possible to clearly determine the parameters of the Plaxis MCC model with these material properties accessed in the field. Yoo et al. (2007) [23] and Yoo and Kim (2009) [24] refer to the Malaysian clay in the study of Tan et al. (2008) [25], located in the region close to Raju (1997) study, in the validation of their finite element analysis. For this reason, soil properties determined in the Raju (1997) field study were converted into MCC material model parameters with the help of these studies [23-25] (Table 1).

At the measurement point in Kebun where the embankment height is 2.6 m, a settlement of about 40 cm has been measured (it should be kept in mind that the soil and stone column layout is different at the sites and the settlement magnitudes cannot be directly compared).

Here, only 25% of the settlement has taken place during embankment construction. The remaining settlement has taken place over a period of almost 8 months thereafter. In areas not treated with vibro replacement, settlements over 1.0 m were measured for comparable embankment heights and soil conditions. The load value corresponding to 2.6 m fill height was used as model loading in the validation study (50 kPa).

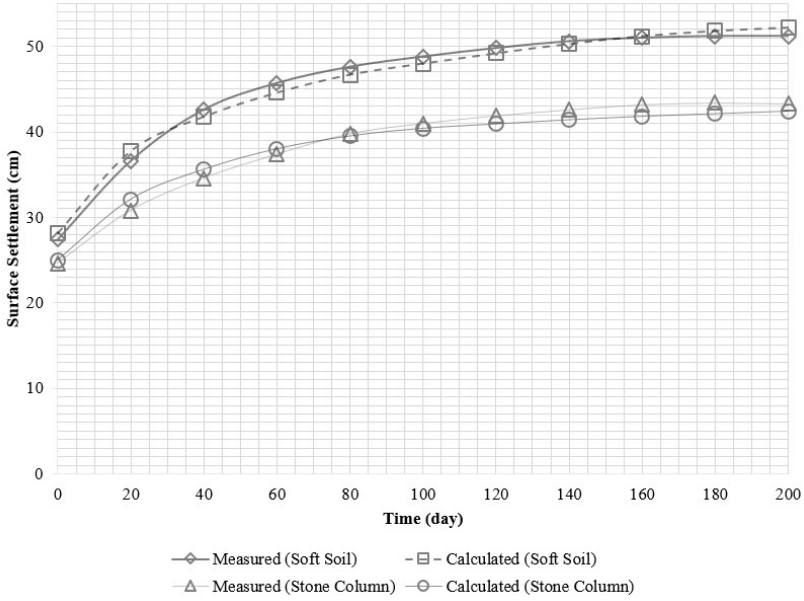

Fig. 2 - Comparison of Measured vs. Calculated Settlements of Soft Soil and Stone Column

The settlement results and the vertical stress transferred to both the column and the soft ground obtained from the numeric study were compared with those measured at the Kebun project (Fig. 2). Consistency between the measured settlement values from the Kebun, Malaysia project and calculated results from the above-mentioned analyses makes the numerical model convenient to apply to parametric studies.

2.4. Numerical Analyses

At first, to choose the most suitable column profile to be used in analyses, column diameter (D) was pre-selected as 0.60 meters and a relative settlement diagram was drawn for the increasing load for both drained and undrained conditions. Relative settlement can be described as the ratio of the settlements between the top of the stone column and the soft clay layer. In line with the experimental study of Debnath and Dey (2017) pressure causing a settlement of 20% of the diameter of the column was considered as the ultimate load-carrying capacity [29]. A uniform load was applied on sand mat until achieving this settlement value. Bearing capacity corresponding to the relative settlement of 20% D was determined as 165 kPa (Fig. 3).

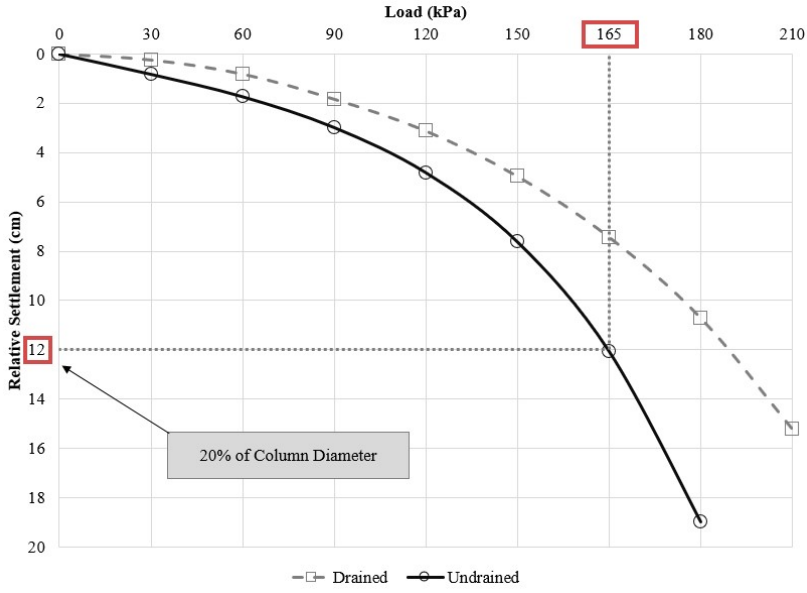

Fig. 3 - Load - Relative Settlement Relationship

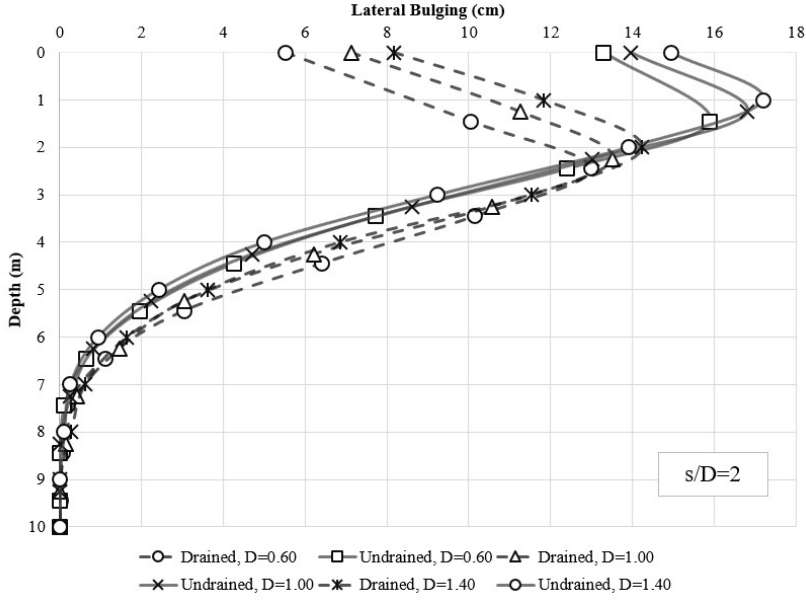

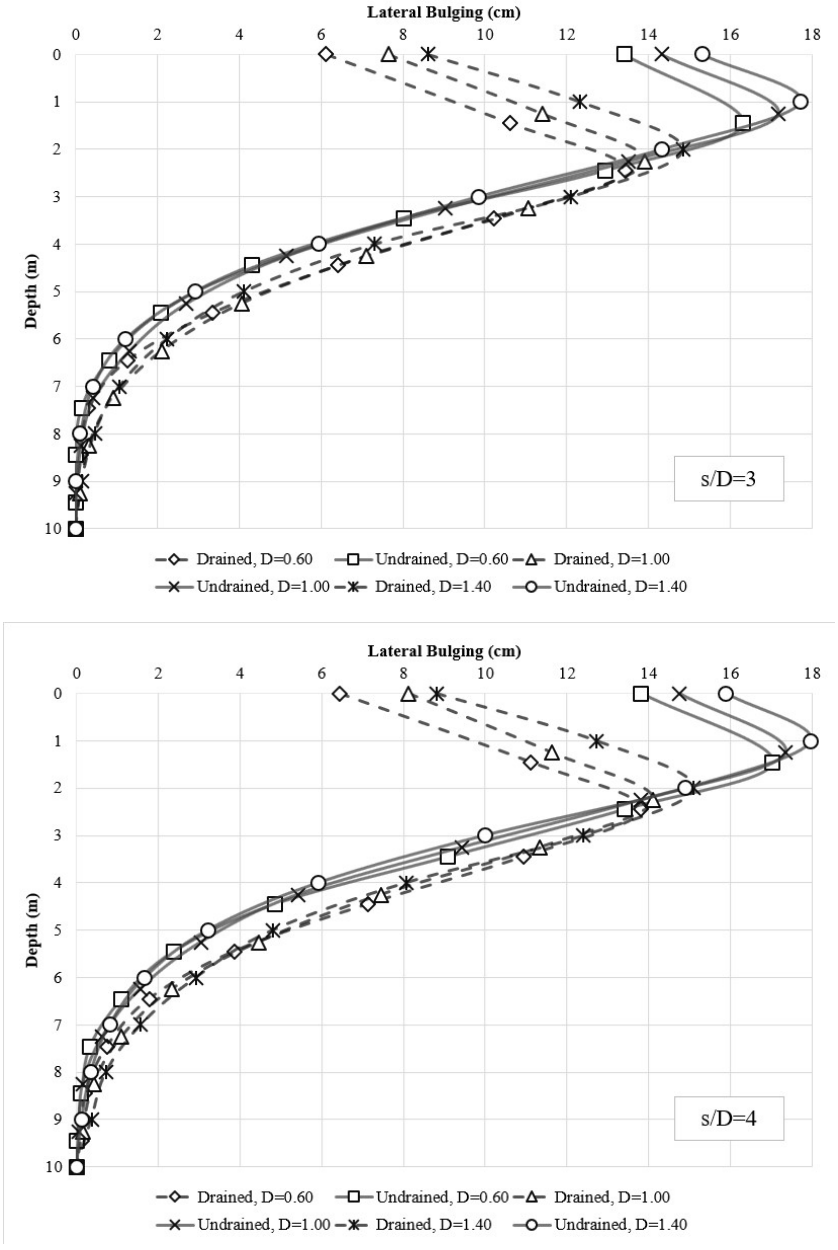

Fig. 4 - Bulging - Depth Relationship (a) s/D=2, (b) s/D=3, (c) s/D=4

This capacity was decided to be used in the following analyses. Then, the stone column variations of 0.60 m, 1.00 m, and 1.40 m diameters (D) and spacing ratios (s/D) of 2, 3, and

4 have been subjected to 165 kPa for both drained and undrained conditions, lateral deformation-depth diagrams were drawn and the maximum bulging values were noted on Fig. 4(a), Fig. 4(b) and Fig. 4(c).

Noted numerical data were reflected on the maximum lateral deformation-spacing ratio diagram (Fig. 5). In order to dilute the effect of column diameter and column spacing, the stone column profile with the least deviation was determined to be D=1.00 m and s/D=3 at undrained condition (UC) and it was decided to be used in the following analyses within the study. This way the stone columns were isolated from lateral/vertical deformation change depending on column diameter or column spacing and bearing capacity change caused by soil arching.

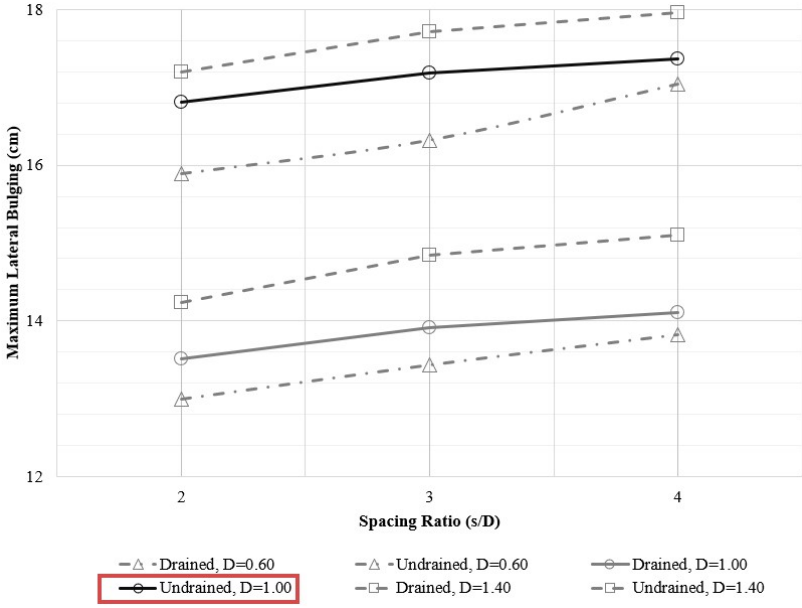

Fig. 5 - Maximum Lateral Deformation - Spacing Ratio (sD) Relationship

Contrary to expectation, undrained settlement values are higher than drained settlement values as can be seen from Fig.5. A similar situation has been observed in previous studies and explained as follows. The consolidation of the soft soil surrounding the stone column can significantly affect both the response of the soil to loading and the load distribution between the column and the soil. The drainage of the column and the instantaneous dissipation of the excess pore-water pressure in the column causes an immediate load transfer to the column. During consolidation, there is a progressive load transfer from the soil to the column. And also, with a continuous consolidation of the soil, which is accelerated by the drainage effect of the columns, an improvement of the soil parameters of the in-situ soil becomes effective [30-31].

The varying material properties and reinforcement scenarios evaluated in the parametric study were summarized in Table 2.

Table 2 - Parameters evaluated in the parametric analyses

Parameter	
Soft soil layer height (H) (m)	10, 11, 12, 13, 14, 15, 16, 18, 20
Column diameter (m)	0.60, 1.00, 1.40
Spacing ratio (s/D)	2, 3, 4
Sand mat thickness (m)	0.00 D, 0.05 D, 0.10 D, 0.15 D, 0.20 D
Geogrid stiffness (J) (kN/m)	1000, 2000, 3000, 4000, 5000, 6000, 7000
Geotextile stiffness (E) (kN/m)	500, 1000, 1500, 2000, 2500, 3000, 3500

3. RESULTS AND DISCUSSIONS

3.1. Effect of Sand Mat Thickness

An unreinforced sand mat layer (USM) that has a thickness varying between 0.0 D to 0.2 D with 0.05 D intervals was deployed on an OSC reinforced soft clay ground. While determining the sand mat thickness, the values given in the Dutch Design Guideline CUR226 [31] were considered. The sand mat layer was designated as two layers in order to lay the

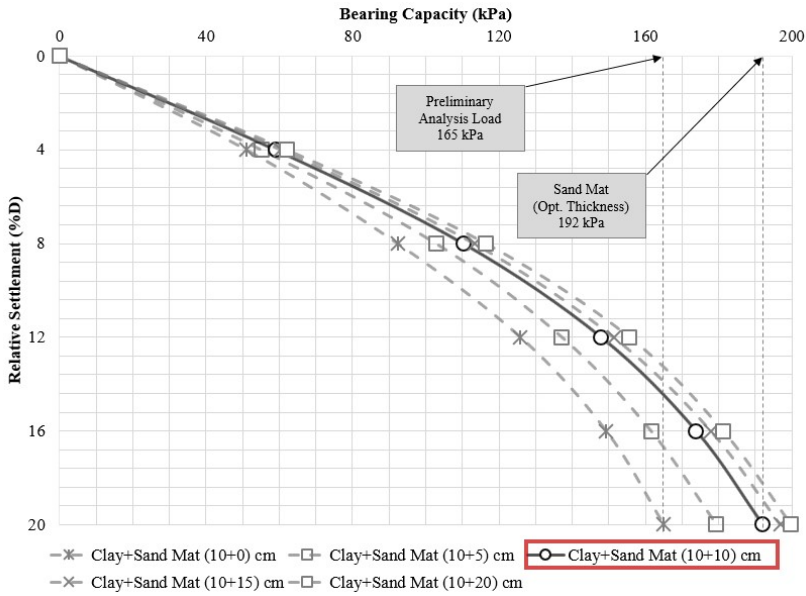

Fig. 6 - Bearing Capacity - Relative Settlement Diagram for Sand Mat Thickness

reinforcement material between these layers e.g., 0.10 D thick sand + geotextile reinforcement + 0.05 D thick sand for a 0.15 D meters thick sand mat. A series of numerical analyses were carried out and bearing capacity-relative settlement diagrams were drawn using the data obtained (Fig. 6).

Sand mat thickness appears to be improving the bearing capacity obviously until 0.2 D meters and beyond that, the effect is not obvious. A sand mat layer of 0.2 D thick was selected as the optimum sand mat and decided to be used at the continuing steps of the numerical study. An early study by Debnath and Dey (2017) indicates that a USM thickness of about 0.2 times the diameter of the footing (i.e., 0.2D) gives the maximum performance improvement in composite foundation systems [29]. The calculated sand mat thickness conforms to the referent study. The selected optimum sand mat was calculated to be causing an increase up to 1.16-fold on the bearing capacity of OSC installed in soft ground.

3.2. Effect of Geogrid Reinforcement Stiffness

The optimum sand mat of 0.2 D meters thick was reinforced with varying axial stiffness (J) of the geogrid reinforcement material; 1000, 2000, 3000, 4000, 5000, 6000, and 7000 kN/m representing a scale of low to very high strength geosynthetic material. Bearing capacity-relative settlement diagrams were drawn using the data obtained from the series of numerical analyses (Fig. 7).

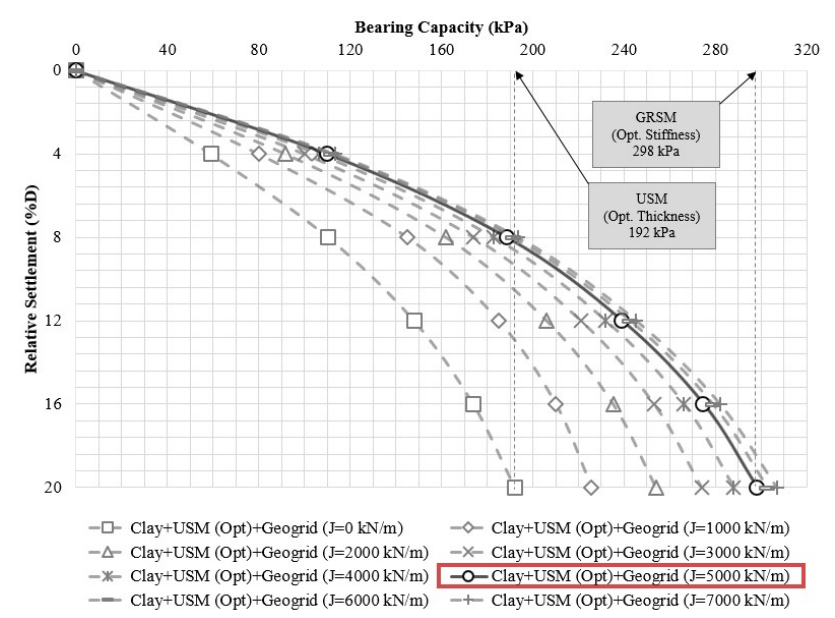

Fig. 7 - Bearing Capacity - Relative Settlement Diagram for Geogrid Stiffness

According to Fig. 7, bearing capacity increases with the increasing stiffness values of geogrid reinforcement until J=5000 kN/m. The improvement becomes insignificant after that level.

Similar results have also been reported in former studies [32-33]. Geogrid reinforcement with 5000 kN/m stiffness was selected as optimum and decided to be used in the ongoing numerical study. The selected optimum GRSM was calculated to be increasing the bearing capacity of the soft ground up to 1.55-fold and 1.81-fold compared to OSC+USM and OSC, respectively.

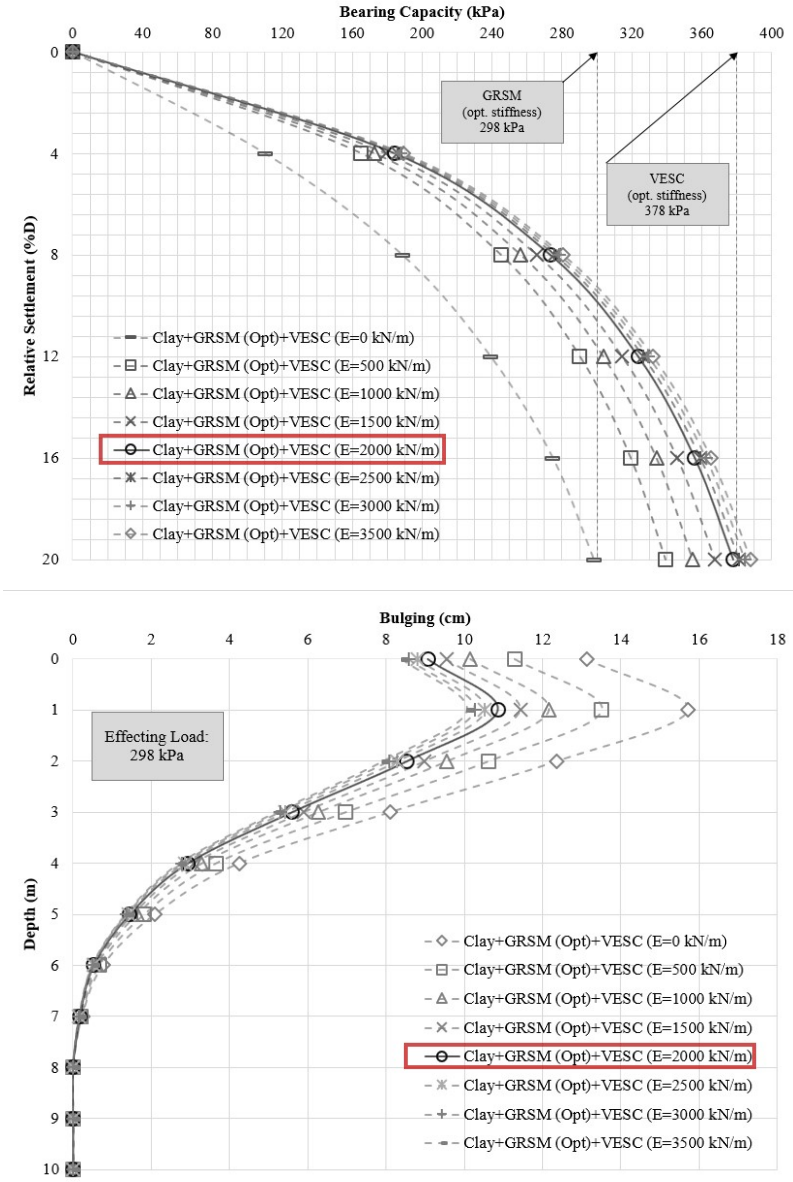

Fig. 8 - Diagrams for Geotextile Stiffness
(a) Bearing capacity-relative settlement, (b) Lateral deformation-depth

3.3. Effect of Geotextile Encasement Stiffness

The OSCs installed in the soft ground under optimum GRSM (m=0.2 D and J=5000 kN/m) were encased with varying axial stiffness of geotextile material; 500, 1000, 1500, 2000, 2500, 3000, and 3500 kN/m representing a scale of low to very high strength geosynthetic material. The lateral deformation of the stone column was not measured in the Raju (1997) field study used for validation. In this numerical study, the lateral deformation of the stone column was calculated as the lateral deformation of the geosynthetic encasement. Bearing capacity-relative settlement diagram Fig. 8(a) and lateral deformation-depth diagram Fig. 8(b) were drawn, respectively by using the data obtained from the series of numerical analyses performed.

According to Fig. 8(a) and Fig. 8(b), additional confinement due to the increasing stiffness of the geosynthetic encasement material appears to be significantly contributing to both the ultimate load capacity and the bulging reduction. The contribution is obvious until the stiffness value of E=2000 kN/m and beyond that enhancement is insignificant. For that matter, a stiffness value of 2000 kN/m for vertical encasement was chosen as optimum and decided to be used at continuing steps of the numerical study. The selected optimum GRSM+VESC was calculated to be increasing the load-carrying capacity of the soft ground up to 1.27-fold, 1.97-fold, and 2.29-fold compared to GRSM+OSC, USM+OSC, and OSC and reducing the lateral deformation up to 31% compared to GRSM+OSC, respectively. Former studies conform the load-carrying capacity improvement and settlement reduction of SCs to the provision of the geosynthetic encasement [29, 34-37].

3.4. Effect of Geotextile Encasement Length

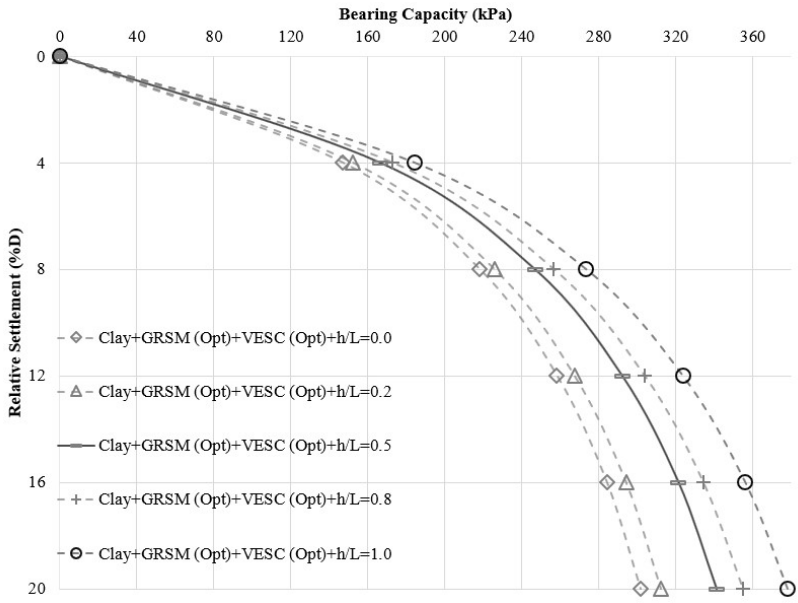

Fig. 9 - Bearing Capacity - Relative Settlement Diagram for Varying Encasement Lengths

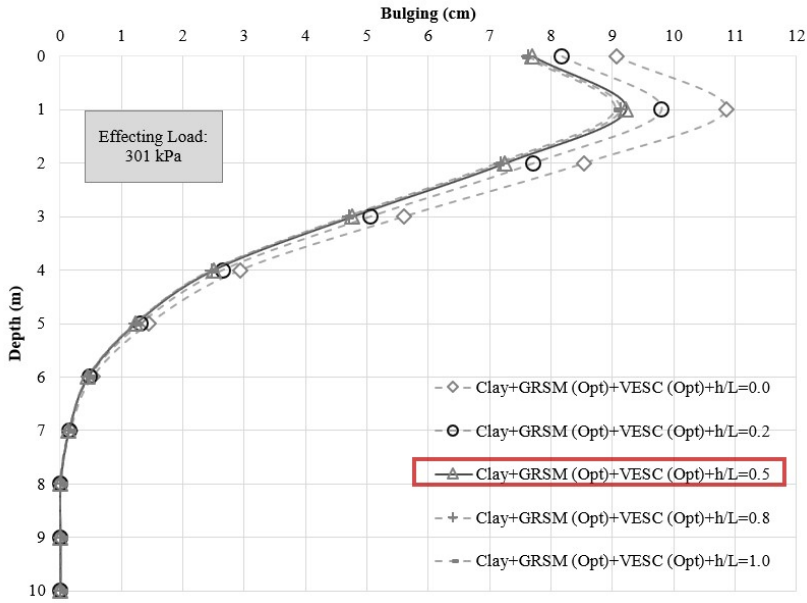

Fig. 10 - Lateral Deformation - Depth Diagram for Varying Encasement Lengths

The analyses on optimized GRSM reinforced (m=0.2 D and J=5000 kN/m) and VESC (E=2000 kN/m) improved soil model were repeated for different encasement lengths of which the ratio of vertical encasement length to column length (h/L) varied 0.0 to 1.0. Bearing capacity-relative settlement (Fig. 9) and lateral deformation-depth diagrams (Fig. 10) were drawn using the data obtained from analyses.

Fig. 9 and 10 show that a vertical encasement from the top to the middle of the column (h/L=0.5) appears to be obviously contributing to both the bearing capacity and the bulging reduction of SC under GRSM. For lengths beyond the middle of the column, the encasement's contribution is insignificant. The bulging is still the main reason for failure of GESC independent to different encasement lengths. Similar results have been reported in former studies. Malarvizhi and Ilamparuthi (2007) indicate that the maximum bulging occurs at 4D from the top of the column [34]. Ali et al. (2012) reveals that whether floating or end-bearing long unreinforced stone columns always fail by bulging whereas short floating columns always fail because of punching. Their study refers that encasement over full column length gives higher failure stress than encasement over the top half or quarter of the column length and also the higher failure stress still occurs at the upper half of the column [35].

Despite the fact of 50% encasement length reduction as a result of encasing the upper half of the stone column, the decrease of bearing ratio of composite ground is determined as 10%. This suggests that the stone column can be encased partially on the condition of reinforcing up to where lateral deformation is maximum. Tandel et al. (2012) imply a 14% decrease in maximum load capacity despite the 50% decrease at encasement length [36]. The calculated load-carrying performance of partially encased stone columns conforms to the referent study.

4. CONCLUSIONS

The conclusions of the study are summarised respective to the analyses order:

(1) Composition of a sand mat at the base of the embankment reduces the settlement difference between the stone column and the soft ground. Sand mat thickness appears to be improving the bearing capacity obviously until 0.2D. The effect becomes insignificant beyond that depth.

(2) Utilizing a layer of geogrid reinforcement in the sand mat increases the effect up to the axial stiffness of J=5000 kN/m. The optimum GRSM (0.2D thick and reinforced by a J=5000 kN/m geogrid layer) caused an increase up to 1.16-fold on the bearing capacity of OSC installed in soft ground.

(3) Geosynthetic encasement can significantly alter the stress/settlement response of the stone column. Besides, encasing the stone columns with a geotextile reduces the lateral displacements. Geotextile encasement up to the stiffness of E=2000 kN/m appears to be the optimum, behind that contribution is insignificant. The optimum GRSM+VESC (vertically encased by a geotextile of E=2000 kN/m stiffness) caused increasing the ultimate load capacity of the soft soil up to 1.27-fold, 1.97-fold, and 2.29-fold compared to GRSM+OSC, USM+OSC, and OSC and reducing the lateral deformation up to 31% compared to GRSM+OSC, respectively.

(4) For end-bearing (fixed) stone columns, an encasement length of 0.5L appears to be contributing significantly to both the bearing capacity and the bulging reduction of SC under GRSM. For lengths beyond the middle of the column, the encasement's contribution is not obvious.

Nomenclature

D	Column Diameter
L	Column Length
φ'	Dilation Angle
c'	Effective Cohesion
ϕ'	Effective Friction Angle
γ'	Effective Unit Weight
E	Elastic Modulus
J	Geogrid Stiffness
E	Geotextile Stiffness
k	Permeability
υ	Poisson's Ratio
K	Slope of Swelling Line
M	Slope of the Critical State Line
λ	Slope of the Virgin Consolidation Line

H	Soft Clay Layer Height
s	Stone Column Spacing
e	Void Ratio at Unit Pressure

References

[1] Borges, J. and Marques, D., Geosynthetic-Reinforced and Jet-Grout Column Supported Embankments on Soft Soils: Numerical Analysis and Parametric Study. Computers and Geotechnics, 38(7):883-896, 2011. DOI: 10.1016/j.compgeo.2011.06.003

[2] Hughes, J., Withers, N. and Greenwood, D.A., A Field Trial of the Reinforcing Effect of a Stone Column in Soil. Géotechnique, 25(1):31-44, 1975. DOI: 10.1680/geot.1975.25.1.31

[3] Madhav, M.R. and Vanitha, L., Analysis and Design of Granular Pile Reinforced Ground. Proceedings of ATC-7 Workshop on Stone Column in Soft Deposits, Korea, Busan:1–17, 2006.

[4] Van Impe, W. and Silence, P., Improving of the Bearing Capacity of Weak Hydraulic Fills by Means of Geotextiles. Proceedings of the 3rd International Conference on Geotextiles, Austria: Vienna:1411-1416, 1986.

[5] Raithel, M., Kempfert, H.G. and Kirchner, A., Geotextile-Encased Columns (GEC) for Foundation of a Dike on very Soft Soils. Proceedings of the 7th ICG International Conference on Geosynthetics, France, Nice:1025-1028, 2002.

[6] Murugesan, S. and Rajagopal, K., Model Tests on Geosynthetic Encased Stone Columns. Geosynthetics International, 14(6):346-354, 2007. DOI: 10.1680/gein.2007.14.6.346

[7] Liu, H., Ng, C.W.W. and Fei, K., Performance of a Geogrid-Reinforced and Pile Supported Highway Embankment over Soft Clay: Case Study. Journal of Geotechnical and Geo-Environmental Engineering, 133(12):1483-1493, 2007. DOI: 10.1061/(ASCE)1090-0241(2007)133:12(1483)

[8] Murugesan, S. and Rajagopal, K., Studies on the Behaviour of Single and Group Geosynthetic Encased Stone Columns. The Journal of Geotechnical and Geo-Environmental Engineering, 136(1):129-139, 2010. DOI: 10.1061/(ASCE)GT.1943-5606.0000187

[9] Yoo, W., Kim, B. and Cho, W., Model Test Study on the Behaviour of Geotextile-Encased Sand Pile in Soft Clay Ground. KSCE Journal of Civil Engineering, 19(3):592-601, 2015. DOI: 10.1007/s12205-012-0473-4

[10] Murugesan, S. and Rajagopal, K. Geosynthetic-Encased Stone Columns: Numerical Evaluation. Geotextiles and Geomembranes, 24(6):349-358, 2006. DOI: 10.1016/j.geotexmem.2006.05.001bulging

[11] Yoo, C., Settlement Behaviour of Embankment on Geosynthetic-Encased Stone Column Installed Soft Ground - A Numerical Investigation. Geotextiles and Geomembranes, 43:484-492, 2015. DOI: 10.1016/j.geotexmem.2015.07.014

[12] Tabesh, A. and Poulos, H., Design Charts for Seismic Analysis of Single Piles in Clay. Geotechnical Engineering, 160(2):85-96, 2007. DOI: 10.1680/geng.2007.160.2.85

[13] Lu, Y., Abusharar, S., Zheng, J., Chen, B. and Yin, J., The Performance of an Embankment on Soft Ground Reinforced with Geosynthetics and Pile Walls. Geosynthetics International, 16:173-182, 2009. DOI: 10.1680/gein.2009.16.3.173

[14] Briançon, L. and Simon, B., Performance of Pile Supported Embankment over Soft Soil: Full-Scale Experiment. Journal of Geotechnical and Geo-Environmental Engineering, 138(4):554-561, 2012. DOI: 10.1061/(ASCE)GT.1943-5606.0000561

[15] Jelušič, P. and Žlender, B., Optimal Design of Reinforced Pad Foundation and Strip Foundation. International Journal of Geomechanics, 18(9), 2018. DOI: 10.1680/jgein.17.00039

[16] Cheng, Q., Wu, J., Zhang, D. and Ma, F., Field Testing of Geosynthetic-Reinforced and Column-Supported Earth Platforms Constructed on Soft Soil. Frontiers of Structural and Civil Engineering, 8(2):124-139, 2014. DOI: 10.1007/s11709-014-0255-9

[17] Liu, W., Qu, S., Zhang, H. and Nie, Z., An Integrated Method for Analysing Load Transfer in Geosynthetic-Reinforced and Pile-Supported Embankment. KSCE Journal of Civil Engineering, 21(3):687-702, 2017. DOI: 10.1007/s12205-016-0605-3

[18] Brinkgreve, R.B.J., Engin, E. and Swolfs, W.M., Plaxis 3D 2012 Manual. Plaxis bv, the Netherlands, 2012.

[19] Raju, V.R., The Behavior of very Soft Cohesive Soils Improved by Vibroreplacement. Ground Improvement Geosystems – Densification and Reinforcement. Thomas Telford, 253-259, 1997. DOI: 10.1680/gigdar.26056.0032

[20] Kaliakin, V., Khabbazian, M. and Meehan, C., Modelling the Behaviour of Geosynthetic Encased Columns: Influence of Granular Soil Constitutive Model. International Journal of Geomechanics, 12(4):357–369, 2012. DOI: 10.1061/(ASCE)GM.1943-5622.0000084

[21] Khabbazian, M., Kaliakin, V. and Meehan, C., Column Supported Embankments with Geosynthetic Encased Columns: Validity of the Unit Cell Concept. Geotechnical and Geological Engineering, 33:425-442, 2015. DOI: 10.1007/s10706-014-9826-8

[22] Ambily, A. and Gandhi, S., Behaviour of Stone Columns Based on Experimental and FEM Analysis. Journal of Geotechnical and Geo-Environmental Engineering, 133(4):405-415, 2007. DOI: 10.1061/(ASCE)1090-0241(2007)133:4(405)

[23] Yoo, C., Song, A.R., Kim, S.B., and Lee, D.Y., Finite Element Modelling of Geogrid-Encased Stone Column in Soft Ground. Geotechnical Society, 23 (10):133-150, 2007.

[24] Yoo, C. and Kim, S.B., Numerical Modeling of Geosynthetic-Encased Stone Column-Reinforced Ground. Geosynthetics International, 16 (3):116-126, 2009. DOI: 10.1680/gein.2009.16.3.116

[25] Tan, S.A., Tjahyono S. and Oo, K.K., Simplified Plane-Strain Modelling of Stone-Column Reinforced Ground. Journal of Geotechnical and Geoenvironmental Engineering, 134 (2):185-194, 2008. DOI: 10.1061/(ASCE)1090-0241(2008)134:2(185)

[26] Almeida, M., Hosseinpour, I., Riccio, M. and Alexiew, D., Behaviour of Geotextile Encased Granular Columns Supporting Test Embankment on Soft Deposit. Geotechnical and Geo-Environmental Engineering, 141(3), 2015. DOI: 10.1061/(ASCE)GT.1943-5606.0001256.

[27] Elias, V. Welsh, J. Warren, J., Lukas, R., Collin, G. Berg, R. R., Ground Improvement Methods, Vol. II. Federal Highway Administration, Washington, DC, USA, FHWA-NHI-06-020, 2006.

[28] Abu-Farsakhl, M., Coronel, J., Tao, M., Effect of Soil Moisture Content and Dry Density on Cohesive Soil–Geosynthetic Interactions Using Large Direct Shear Tests, Journal of Materials in Civil Engineering, 19 (7):540-549, 2007. DOI:10.1061/(ASCE)0899-1561(2007)19:7(540).

[29] Debnath, P. and Dey, A., Bearing Capacity of Geogrid Reinforced Sand over Encased Stone Columns in Soft Clay. Geotextiles and Geomembranes, 45:653-665, 2017. DOI: 10.1016/j.geotexmem.2017.08.006

[30] Juran, I. and Guermazi, A., Settlement Response of Soft Soils Reinforced by Compacted Sand Columns. Journal of Geotechnical Engineering, 114 (8):930-943, 1988. DOI: 10.1061/(ASCE)0733-9410(1988)114:8(930)

[31] Van Eekelen, S.J.M. and Brugman, M.H.A., Design Guideline Basal Reinforced Piled Embankments. CRC Press, SBR Kennisoverdracht B.V., 2016.

[32] Zhang, N. et al., Evaluation of Effect of Basal Geotextile Reinforcement under Embankment Loading on Soft Marine Deposits. Geotextiles and Geomembranes, 43(6):506-514, 2015. DOI: 10.1016/j.geotexmem.2015.05.005

[33] Kahyaoğlu, M.R. and Vaníček, M.A., Numerical Study of Reinforced Embankments Supported by Encased Floating Columns. Acta Geotechnica Slovenica, 16(2):25-38, 2019. DOI: 10.18690/actageotechslov.16.2.25-38.2019

[34] Malarvizhi, S. and Ilamparuthi, K., Comparative Study on the Behaviour of Encased Stone Column and Conventional Stone Column. Soils and Foundations, 47(5):873-885, 2007. DOI: 10.3208/sandf.47.873

[35] Ali, K., Shahu, J. and Sharma, K., Model Tests on Geosynthetic-Reinforced Stone Columns: A Comparative Study. Geosynthetics International, 19(4):292-305, 2012. DOI:10.1680/gein.12.00016

[36] Tandel, Y. and Solanki, C.H., Deformation Behaviour of Ground Improved by Reinforced Stone Columns. Australian Geomechanics Journal, 47:51-59, 2012.

[37] Xu, Z., Sathiyamoorthy, R., Jian-Feng, C., Zhen, Z. and Liang-Yong, L., 3D Coupled Mechanical and Hydraulic Modelling of Geosynthetic Encased Stone Column-Supported Embankment Over Soft Clay. Marine Georesources & Geotechnology, 2020, DOI:10.1080/1064119X.2020. 1825571